

Experimental Investigations and Ab Initio Studies of Tellurium(II) Dithiolates, Te(SR)₂Holger Fleischer,^{*,†} Sandra Stauf,[†] and Dieter Schollmeyer[‡]

Institut für Anorganische Chemie und Analytische Chemie and Institut für Organische Chemie, Universität Mainz, Duesbergweg 10–14, D-55099 Mainz, Germany

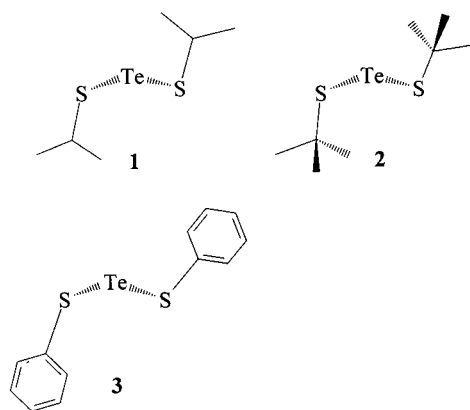
Received January 21, 1999

The reaction between Te(OⁱPr)₄ and HSR offers a new and effective route to tellurium dithiolates, Te(SR)₂. Te(SⁱPr)₂ (**1**) and Te(SⁱBu)₂ (**2**) are stable compounds whereas Te(SPh)₂ (**3**) slowly decomposes at room temperature to give Te and Ph₂S₂. IR spectra of **1–3** and ab initio calculations (HF/3-21G(d) and MP2 with double- ζ polarization effective core potential basis set) show $\nu_{\text{as}}(\text{Te-S})$ and $\nu_{\text{s}}(\text{Te-S})$ to be around 340 and 380 cm⁻¹, respectively. UV spectra exhibit similar λ_{max} (346–348 nm) for all three compounds, with the greater extinction coefficient of **3** accounting for its different and more intense color. Analysis of the molecular orbitals of the model compound Te(SCH₃)₂ shows that the phototransition is likely to be of n_p(Te)– $\sigma^*(\text{Te-S})$ type, thus rationalizing the instability of **3** when irradiated. Single-crystal X-ray diffraction of **1–3** revealed the following basic structural parameters: **1** $d_{\text{av}}(\text{Te-S})$ 239.4(1) and $d_{\text{av}}(\text{S-C})$ 183.8(5) pm, $\angle(\text{STeS})$ 99.61(4) and $\angle_{\text{av}}(\text{TeSC})$ 105.8(3)°, $\tau(\text{CSTeS})$ 77.0(2) and 90.3(2)°; **2** $d(\text{Te-S})$ 239.1(1) and $d(\text{S-C})$ 186.4(2) pm, $\angle(\text{STeS})$ 103.88(2) and $\angle(\text{TeSC})$ 107.6(1)°, $\tau(\text{CSTeS})$ 78.01(8)°; **3** $d(\text{Te-S})$ 240.6(2) and $d(\text{S-C})$ 177.4(7) pm, $\angle(\text{STeS})$ 100.12(6)° $\angle(\text{TeSC})$ 103.2(2)°, $\tau(\text{CSTeS})$ 69.0(3) and $\tau(\text{CCSTe})$ 81.6(6)°. Geometries of model compounds Te(SH)₂ and Te(SCH₃)₂ optimized at the MP2 level exhibit $d(\text{Te-S})$, $\angle(\text{STeS})$, and $\tau(\text{XSTeS})$ (X = H, C) values similar to those of **1–3**. Natural bond orbital analysis revealed n_p(S¹)– $\sigma^*(\text{Te-S}^2)$ hyperconjugation as the cause for the CSTeS torsion angles being close to 90 or –90°. Thermochemical calculations on the HF and MP2 level proved Te(SH)₄ to be unstable with respect to Te(SH)₂ and HSSH, thus rationalizing the reduction of Te(IV) to Te(II) when Te(OⁱPr)₄ or TeO₂ are reacted with thiols. NMR spectra reveal ligand exchange reactions between different tellurium(II) dithiolates and between Te(SR)₂ and HSR'. These types of reaction offer other routes to tellurium(II) dithiolates.

Introduction

The reaction of Te(IV) compounds with thiols recently gained interest due to the inhibitive properties of ammonium trichloro-(dioxoethylene-O,O')tellurate (AS101) and others on cysteine proteases.¹ If Te(IV) compounds are reacted with thiols, reduction of Te(IV) to Te(II) occurs.^{2,3} The recently claimed synthesis of a tellurium(IV) tetrathiolate⁴ is not unequivocal, since no structural or ¹²⁵Te NMR data are presented. While the reaction of Te(IV) compounds with thiols is not only of chemical but also biochemical and pharmaceutical interest, little is known about the chemistry or the spectroscopic and structural properties of Te(SR)₂.⁵ The only structurally characterized tellurium(II) dithiolate known to us is Te(SCPh₃)₂.⁶ In contrast to Te-[N(CH₃)₂]₂ which is polymeric in the solid state,⁶ Te[SCPh₃]₂ was found to be monomeric.

In the present study, we explored the chemistry, spectroscopy, molecular structures, and bonding properties of tellurium(II) dithiolates by experimental methods and ab initio calculations.

Figure 1. Structural formulas of compounds **1–3**.

Results and Discussion

Synthesis. The tellurium(II) dithiolates Te(SⁱPr)₂ (**1**), Te(SⁱBu)₂ (**2**), and Te(SPh)₂ (**3**) (Figure 1) can readily be prepared in good yields from Te(OⁱPr)₄⁷ and the corresponding thiols, according to eq 1 (R = ⁱPr, ⁱBu or Ph):⁸



The advantage of Te(OⁱPr)₄ over TeO₂² in the synthesis of Te(SR)₂ is attributed to the homogeneous reaction in the present case. The immediate appearance of the characteristic colors of

(7) Denney, D. B.; Denney, D. Z.; Hammond, P. J.; Hsu, Y. F. *J. Am. Chem. Soc.* **1981**, *103*, 2340–2347.

[†] Institut für Anorganische Chemie und Analytische Chemie.

[‡] Institut für Organische Chemie.

(1) Albeck, A.; Weitman, H.; Sredni, B.; Albeck, M. *Inorg. Chem.* **1998**, *37*, 1704–1712.

(2) Mazurek, W.; Moritz, A. G.; O'Connor, M. J. *Inorg. Chim. Acta* **1986**, *113*, 143–146.

(3) Stukalo, E. A.; Yur'eva, E. M.; Markovskii, L. N. *Zh. Org. Khim.* **1983**, *19*, 343–346.

(4) Ogawa, S.; Yamashita, M.; Sato, R. *Tetrahedron Lett.* **1995**, *36*, 587–590.

(5) Chivers, T. *J. Chem. Soc., Dalton Trans.* **1996**, 1185–1194.

(6) Allan, R. E.; Gornitzka, H.; Kärcher, J.; Paver, M. A.; Rennie, M. A.; Russell, C. A.; Raitby, P. R.; Stalke, D.; Steiner, A.; Wright, D. W. *J. Chem. Soc., Dalton Trans.* **1996**, 1727–1730.

Table 1. Experimental and Calculated $\nu(\text{Te-S})$ Bond Stretching Frequencies for **1–3** and $\text{Te}(\text{SCH}_3)_2$

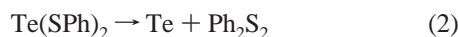
1	2	3	$\text{Te}(\text{SCH}_3)_2^a$	mode
380(s)	386(s)		367.8 (2.337)	$\nu_s(\text{Te-S})$
350(w)	349(s)	336(s)	351.5 (22.842)	$\nu_{as}(\text{Te-S})$

^a Unscaled MP2/LANL2DZP frequencies and intensities (km mol^{-1} , in parentheses) are given.

the tellurium(II) dithiolates when $\text{Te}(\text{O}^i\text{Pr})_4$ is added to a solution of HSR indicates that substitution of $-\text{O}^i\text{Pr}$ by $-\text{SR}$ and reduction of Te(IV) to Te(II) are both quick reactions. The instability of a possible intermediate $\text{Te}(\text{SR})_4$ toward decomposition into $\text{Te}(\text{SR})_2$ and S_2R_2 was shown by thermochemical calculations (see Molecular Structures and Thermochemical ab Initio Calculations).

Recrystallization from methanol yielded pure $\text{Te}(\text{SR})_2$. The derivatives **1** and **2** precipitated as yellow needlelike crystals, while **3** formed deep red crystals. They are very soluble in nonpolar solvents, slightly soluble in methanol, and insoluble in water.

While **1** and **2** are stable at room temperature for several days and melt without decomposition, **3** decomposes under these conditions. From a solution of **3** in C_6D_6 , exposed to daylight, a mirror of elemental tellurium formed. Ph_2S_2 was identified by NMR spectroscopy as the byproduct of the reaction, which thus proceeds according to eq 2:



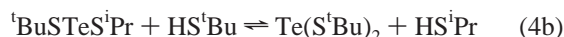
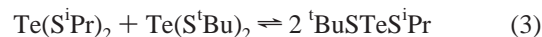
UV Spectra. The UV spectra exhibited λ_{max} at 349.2, 348.7, and 347.7 nm for **1**, **2**, and **3**, respectively, but a much bigger extinction coefficient for **3** ($3750 \text{ cm}^2 \text{ mol}^{-1}$) than for **1** and **2** (593 and $645 \text{ cm}^2 \text{ mol}^{-1}$, respectively). Consequently, the absorption band of **3** extends far more into the visible region of the spectrum than those of **1** and **2**. Thus, the different colors of **1** and **2** (yellow) and **3** (red) are not due to different λ_{max} but to different extinction coefficient. The analysis of the molecular orbitals for $\text{Te}(\text{SCH}_3)_2$ (C_2 -symmetry) reveals that the HOMO (b symmetry) is mainly a p-type lone-pair of the Te atom while the LUMO (b symmetry) represents a $\sigma^*(\text{Te-S})$ orbital. It seems reasonable to attribute the enhanced sensitivity of **3** toward normal daylight to its stronger absorption in the visible region of the spectrum. Promotion of an electron into the $\sigma^*(\text{Te-S})$ -type LUMO weakens the Te-S bond and makes a bond cleavage more likely.

IR Spectra. IR spectra revealed similar wavenumbers for the Te-S bond stretching frequencies, with $\nu_{as}(\text{Te-S})$ being slightly smaller for **3** than for **1** and **2** (see Table 1). Unscaled ab initio calculated MP2/LANL2DZP vibrational frequencies of $\text{Te}(\text{SCH}_3)_2$ reproduce $\nu_{as}(\text{Te-S})$ of **1** and **2** quite well and $\nu_s(\text{Te-S})$ still to a reasonable degree.

NMR Spectra and Ligand Exchange Reactions. Variable-temperature ^1H and ^{13}C NMR spectra of **1** between 25 and -80 °C showed only a slight variation of the chemical shifts, with broader signals at lower temperature. No ^{125}Te satellites due to $^1\text{H}-^{125}\text{Te}$ or $^{13}\text{C}-^{125}\text{Te}$ coupling occurred in any of the ^1H and ^{13}C spectra of **1–3**. Furthermore, the $-\text{CH}(\text{CH}_3)_2$ groups of **1** gave rise to a single resonance for the methyl groups in the ^1H and ^{13}C spectra, which indicates some kind of dynamic

averaging. The four methyl groups in **1** would only be equal if the molecule exhibits C_{2v} symmetry. This geometry was shown to be unfavorable for the model compound $\text{Te}(\text{SH})_2$ (see Molecular Structures and Thermochemical ab Initio Calculations). Assuming C_2 symmetry, the two methyl groups within one $-\text{CH}(\text{CH}_3)_2$ group exhibit different environments, but each of them is equal to one methyl group of the symmetry-related $-\text{CH}(\text{CH}_3)_2$ moiety. The molecular symmetry can be changed to C_s by intramolecular rotation about one Te-S bond, where methyl groups of different $-\text{CH}(\text{CH}_3)_2$ moieties that were equal under C_2 symmetry become different and vice versa. Such a mechanism would be an explanation for the averaging of different chemical environments of the methyl groups. The absence of $^3J(^1\text{H}, ^{125}\text{Te})$ and $^2J(^{13}\text{C}, ^{125}\text{Te})$ coupling cannot be caused by intramolecular rotation, as no bonds are broken. The immediate appearance of a signal of $^i\text{BuTeS}^i\text{Pr}$ in the ^{125}Te NMR spectrum of a 1:1 mixture of **1** and **2** unequivocally proved intermolecular exchange between these molecules. As was already found by Mazurek et al.,² the ^{125}Te NMR shift of $\text{Te}(\text{SR})_2$ compounds varies substantially with R. The effects of both $-\text{SR}$ ligands on $\delta(^{125}\text{Te})$ are additive, as the shift of $^i\text{PrTeS}^i\text{Bu}$ ($\delta = 969.7$) is nearly equal to the arithmetic average of the shifts of **1** ($\delta = 1026.9$) and **2** ($\delta = 906.1$). The ^{125}Te decoupling of the ^1H and ^{13}C NMR spectra can thus readily be rationalized in terms of chemical exchange. No ligand exchange was found between **1** and $\text{Te}(\text{O}^i\text{Pr})_4$ or HO^iPr .

We further investigated ligand exchange between **1** and **2** (eq 3) and between **1** and HS^iBu (eqs 4a and 4b) by means of ^1H and ^{125}Te NMR spectroscopy.



The equilibrium according to eq 3 was reached within minutes after mixing equimolar amounts of **1** and **2** in CDCl_3 , the ^{125}Te NMR intensity ratio $^i\text{BuTeS}^i\text{Pr}:\text{Te}(\text{S}^i\text{Bu})_2 = 1:2:1$ indicating $\Delta G^{298} \approx 0$. In contrast, a mixture of **1** and HS^iBu needed about 12 days to equilibrate according to eqs 4a and 4b. Neglecting the reverse reaction of eq 4a, the second-order rate constant for eq 4a was determined from the ^{125}Te NMR signal intensities 16 h after the reaction was initiated as $k = 1.5 \times 10^{-2} \text{ L h}^{-1} \text{ mol}^{-1}$. Again, the statistical distribution of the ^iPr and ^iBu groups among thiols and tellurium(II) dithiolates suggests ΔG^{298} to be close to zero. This is not surprising since both eqs 3 and 4 are isodesmic and neither enthalpy nor entropy should change substantially with the proceeding of the reactions. In contrast, in the reaction between $\text{Te}(\text{O}^i\text{Pr})_4$ and HO^iBu , the bulky ^iBu group prefers to remain as a free alcohol.⁹ This difference might reflect the enhanced steric repulsion between ligands in $\text{Te}(\text{OR})_4$ compounds compared to the situation in $\text{Te}(\text{SR})_2$. It is not clear if either $-\text{SR}$ or $-\text{R}$ are exchanged in eqs 3 and 4, but it can be inferred from the different reactivities of $\text{Te}(\text{SR})_2$ toward $\text{Te}(\text{SR}')_2$, HSR' , $\text{Te}(\text{OR})_4$ and HOR that the exchange mechanism is not initiated by a heterolytic cleavage of the Te-S bond. Otherwise a reaction between $\text{Te}(\text{SR})_2$ and $\text{Te}(\text{OR})_4$ or HOR should occur and reaction with HSR' should be as fast as with $\text{Te}(\text{SR}')_2$.

(8) A comparative experiment showed that the preparation of **2** from TeO_2 and $^i\text{BuSH}$, as described by Mazurek et al.,² took longer and resulted in lower yields. Reaction of dithioglycol, $\text{HSCH}_2\text{CH}_2\text{SH}$, with $\text{Te}(\text{O}^i\text{Pr})_4$ lead to reduction to elemental Te, and no organotellurium compound could be isolated. As well, no $\text{Te}(\text{SR})_2$ but only elemental tellurium was isolated from the reaction of TeCl_4 and NaSR in ethanol.

(9) Gottlieb, H. E.; Hoz, S.; Elyashiv, I.; Albeck, M. *Inorg. Chem.* **1994**, *33*, 808–811.

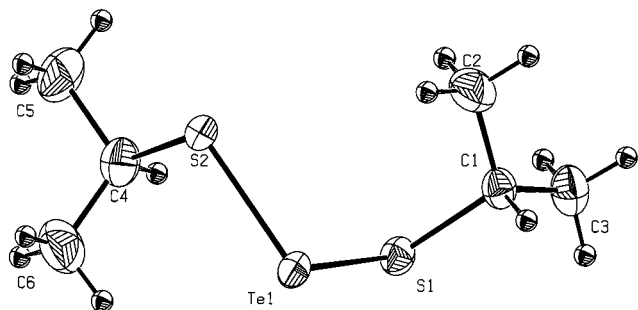


Figure 2. ORTEP diagram of **1**. Displacement ellipsoids are at the 50% probability level. Important structural parameters (distances, pm; angles, deg) of the molecule: $d(\text{Te1}-\text{S1})$ 239.3(1), $d(\text{Te1}-\text{S2})$ 239.5(2), $d(\text{S1}-\text{C1})$ 184.1(4), $d(\text{S2}-\text{C4})$ 183.5(4), $d(\text{C1}-\text{C2})$ 151.2(7), $d(\text{C1}-\text{C3})$ 151.8(7), $d(\text{C4}-\text{C5})$ 153.0(9), $d(\text{C4}-\text{C6})$ 149.3; $\angle(\text{S1Te1S2})$ 99.61(4), $\angle(\text{Te1S1C1})$ 106.1(2), $\angle(\text{Te1S2C4})$ 105.5(2), $\angle(\text{S1C1C2})$ 112.0(3), $\angle(\text{S1C1C3})$ 105.8(3), $\angle(\text{S2C4C5})$ 105.3(3), $\angle(\text{S2C4C6})$ 113.9(3), $\angle(\text{C2C1C3})$ 112.3(4), $\angle(\text{C5C4C6})$ 111.8(5); $\tau(\text{S1Te1S2C4})$ 77.0(2), $\tau(\text{S2Te1S1C1})$ 90.3(2), $\tau(\text{Te1S1C1C3})$ 173.0(3), $\tau(\text{Te1S2C4C5})$ 179.5(4).

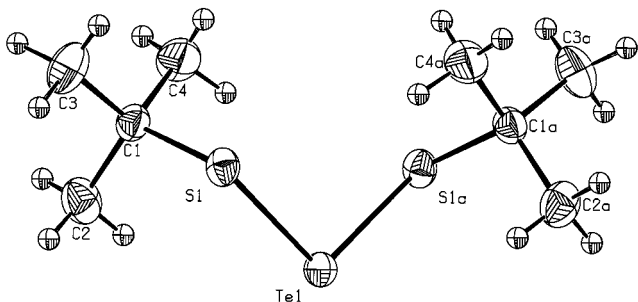


Figure 3. ORTEP diagram of **2**. Displacement ellipsoids are at the 50% probability level. Important structural parameters (distances, pm; angles, deg) of the molecule: $d(\text{Te1}-\text{S1})$ 239.1(1), $d(\text{S1}-\text{C1})$ 186.4(2), $d(\text{C1}-\text{C2})$ 151.8(3), $d(\text{C1}-\text{C3})$ 152.9(4), $d(\text{C1}-\text{C4})$ 151.9(4); $\angle(\text{S1Te1S1a})$ 103.88(2), $\angle(\text{S1Te1C1})$ 107.62(8), $\angle(\text{S1C1C2})$ 111.2(1), $\angle(\text{S1C1C3})$ 103.7(2), $\angle(\text{S1C1C4})$ 109.4(2), $\angle(\text{C2C1C3})$ 110.4(2), $\angle(\text{C2C1C4})$ 111.2(2), $\angle(\text{C3C1C4})$ 110.7(2); $\tau(\text{S1aTe1S1C1})$ 78.01(8), $\tau(\text{Te1S1C1C3})$ 173.3(2).

Molecular Structures and ab Initio Thermochemical Calculations. The molecular structures of **1–3** in the solid state are shown in Figures 2–4. The similarity between **1** and **2** is e.g. well reflected by their basic structural parameters. Furthermore, concerning the comparable structural parameters of **1**, **2** and $\text{Te}(\text{SCH}_3)_2$, the MP2/LANL2DZP-optimized values for $\text{Te}(\text{SCH}_3)_2$ agree well with the experimental XRD values of **1** and **2**. This is consistent with the absence of distorting intermolecular interactions in the crystal structures of **1** and **2**. The absolute values of the torsion angles around the Te–S bonds, i.e., $\tau(\text{CSTeS})$, are approximately between 70 and 100° (see Table 2), a feature that seems to be common not only for compounds $\text{Te}(\text{SR})_2$ but also for compounds containing CSSeS units, e.g., $\text{Se}(\text{SCH}_2\text{CH}_2\text{COOH})_2$ 84.0°,¹¹ $\text{Se}[\text{SC}(\text{O})\text{Ph}]_2$ –87.6°,¹² and $\text{Se}[\text{SC}(\text{O})\text{CH}_3]_2$ 100.3° and –90.8°.¹³ The preference for

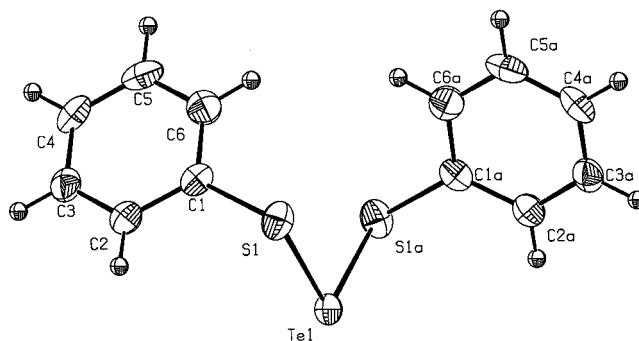
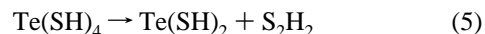


Figure 4. ORTEP diagram of **3**. Displacement ellipsoids are at the 50% probability level. Important structural parameters (distances, pm; angles, deg) of the molecule: $d(\text{Te1}-\text{S1})$ 240.6(2), $d(\text{S1}-\text{C1})$ 177.4(7), $d(\text{C1}-\text{C2})$ 139.7(10), $d(\text{C1}-\text{C6})$ 138.7(11), $d(\text{C2}-\text{C3})$ 138.1(9), $d(\text{C5}-\text{C6})$ 138.7(9), $d(\text{C3}-\text{C4})$ 137.9(11), $d(\text{C4}-\text{C5})$ 137.2(12); $\angle(\text{S1Te1S1a})$ 100.12(6), $\angle(\text{C1S1Te1})$ 103.2(2), $\angle(\text{S1C1C2})$ 121.4(5), $\angle(\text{S1C1C6})$ 119.4(5), $\angle(\text{C6C1C2})$ 119.2(6), $\angle(\text{C3C2C1})$ 119.5(6), $\angle(\text{C4C3C2})$ 120.7(6), $\angle(\text{C3C4C5})$ 120.0(7), $\angle(\text{C4C5C6})$ 120.0(7); $\tau(\text{S1Te1S1aC1})$ 69.0(3), $\tau(\text{Te1S1C1C2})$ 91.5(6), $\tau(\text{S1C1C2C3})$ –177.9(7), $\tau(\text{S1C1C6C5})$ 178.1(7), $\tau(\text{C6C1C2C3})$ 2.8(9), $\tau(\text{C2C1C6C5})$ –2.6(9), $\tau(\text{C2C3C4C5})$ –0.3(9), $\tau(\text{C3C4C5C6})$ 0.5(10), $\tau(\text{C4C5C6C1})$ 1.0(10).

such a conformational arrangement can be rationalized in terms of $n_p(\text{S}^1)-\sigma^*(\text{E}-\text{S}^2)$ hyperconjugation (E = Se, Te) (see further down).

At all levels of calculations applied, the C_{2v} -symmetric structures of all molecules investigated proved to be local minima on the potential energy surface. HF/3-21G(d) C_{2v} -symmetric structures for $\text{Te}(\text{SH})_2$ (“W-shaped”) and $\text{Te}(\text{SH})_4$ (all S–H bond vectors pointing into the semi-space of the lone pair) represent second and fourth order saddle points, respectively, the modes with negative force constants being mainly torsional motions around the Te–S bonds, lowering the symmetry from C_{2v} to C_2 . The HF/3-21G(d) energy difference, $E(C_{2v}) - E(C_2)$, is 57.8 and 58.5 kJ mol^{–1}, for $\text{Te}(\text{SH})_2$ and $\text{Te}(\text{SH})_4$, respectively. Two different starting geometries with the parameter for the torsion angles $\tau(\text{HSTeS})$ being 90.0 and 5.0° were tested for $\text{Te}(\text{SH})_2$ (C_2) and both lead to the same optimized geometry. Second-order perturbation theory analysis of the Fock matrixes in the natural bond orbital basis¹⁴ for $\text{Te}(\text{SCH}_3)_2$ and $\text{Te}(\text{SH})_2$ (C_2) revealed $n_p(\text{S}^1)-\sigma^*(\text{Te}-\text{S}^2)$ hyperconjugation, with total energies (two such interactions per molecule) of 77.8 and 82.4 kJ mol^{–1}, respectively. This hyperconjugation is by far the biggest of all second-order effects for the present Fock matrixes. A similar analysis for $\text{Te}(\text{SH})_2$ with C_{2v} symmetry [$\tau(\text{HSTeS}) = 0^\circ$] led to a total energy of 8.0 kJ mol^{–1} for the same type of interaction. This significant reduction is due to a much smaller intergral overlap between $n_p(\text{S}^1)$ and $\sigma^*(\text{Te}-\text{S}^2)$. Thus $n_p(\text{S}^1)-\sigma^*(\text{Te}-\text{S}^2)$ hyperconjugation stabilizes conformations with $\tau(\text{C}(\text{H})\text{STeS})$ close to 90°. A similar connection was found for the $n_p(\text{N})-\sigma^*(\text{Si}-\text{Cl})$ interaction and the conformation of disilylamines.¹⁵ Additionally, CSTeS or HSTeS torsions close to 90 or –90° minimize the repulsion between the p-type lone pairs of Te and S.

The enthalpy of eq 5 was calculated as –73.3 kJ mol^{–1} (HF/3-21G(d)) and –46.5 kJ mol^{–1} (MP2/LANL2DZP), respectively, thus showing $\text{Te}(\text{SH})_4$ to be thermodynamically unstable. This



is in accordance with the experimental observation that reduction from Te(IV) to Te(II) takes place when OR ligands of $\text{Te}(\text{OR})_4$

(10) Subramanian, I.; Aravamudan, G.; Rout, G. C.; Seshasayee, M. J. *Crystallogr. Spectrosc. Res.* **1984**, *14*, 239–248.

(11) Rao, G. V. N. A.; Seshasayee, M.; Aravamudan, G.; Rao, T. N.; Venkatasubramanian, P. N. *Acta Crystallogr., Sect. B* **1982**, *38*, 2852–2855.

(12) Aravamudan, G.; Subrahmanyam, T.; Seshasayee, M.; Rao, G. V. N. *A Polyhedron* **1983**, *2*, 1025–1029.

(13) Brondmo, N. J.; Esperas, S.; Husebye, S. *Acta Chem. Scand. Ser. A* **1975**, *29*, 93.

(14) Reed, A. E.; Curtiss, L. A.; Weinhold, F. *Chem. Rev.* **1988**, *88*, 899–926.

(15) Fleischer, H.; Brain, P. T.; Rankin, D. W. H.; Robertson, H. E.; Bühl, M.; Thiel, W. *J. Chem. Soc., Dalton Trans* **1998**, 593–600.

Table 2. Comparison of Selected Structural Parameters of Te(SR)₂ Compounds

	$d_{\text{av}}(\text{Te}-\text{S})/\text{pm}$	$d_{\text{av}}(\text{S}-\text{X}^a)/\text{pm}$	$\angle(\text{STeS})^\circ$	$\angle_{\text{av}}(\text{TeSX}^a)^\circ$	$\tau(\text{X}^a\text{STeS})^\circ$
1	239.4(1)	183.8(5)	99.61(4)	105.8(3)	77.0(2)/90.3(2)
2	239.1(1)	186.4(2)	103.88(2)	107.6(1)	78.01(8)
3	240.6(2)	177.4(7)	100.12(6)	103.2(2)	69.0(3)
Te(SCPh ₃) ₂ ^b	237.9(2)	191.8(7)	110.8(1)	113.7(2)	80.2
Te[SC(O)Ph] ₂ ^c	237.2	183.2	103.1	102.6	89.1
Te(SCH ₃) ₂ ^d	239.30	185.18	100.54	102.25	75.88
Te(SH) ₂ ^d	240.17	134.76	102.54	97.68	94.72

^a X = H for Te(SH)₂, else X = C. ^b Values taken from ref 6. ^c Values taken from ref 10. ^d Ab initio (MP2/LANL2DZP) optimized geometry with symmetry restraint to C₂.

Table 3. Crystal Data for Compounds **1–3**^a

	1	2	3
empirical formula	C ₆ H ₁₄ S ₂ Te	C ₈ H ₁₈ S ₂ Te	C ₁₂ H ₁₀ S ₂ Te
fw/g mol ⁻¹	277.90	305.95	345.93
cryst syst	triclinic	monoclinic	orthorhombic
space group	<i>P</i> -1	<i>C</i> 2/ <i>c</i>	<i>Pbcn</i>
<i>Z</i>	2	4	4
temp/K	193	193	194
$\rho_{\text{calc}}/\text{g cm}^{-3}$	1.782	1.645	1.873
<i>a</i> /Å	8.636(2)	16.013(2)	15.598(3)
<i>b</i> /Å	8.677(1)	10.135(2)	10.440(2)
<i>c</i> /Å	8.915(1)	9.037(2)	7.533(3)
α /deg	85.52(1)	90.00	90.00
β /deg	63.67(1)	122.61(1)	90.00
γ /deg	61.30(1)	90.00	90.00
<i>V</i> /Å ³	517.3(2)	1235.4(6)	1226.4(5)
reflms measd	2396	5387 (full sphere)	2122
unique reflms	2242	1350	1340
μ/cm^{-1}	32.10	26.96	27.29
reflms $ F > 4\sigma(F)$	2208	1262	703
<i>R</i> [$ F > 4\sigma(F)$] ^b	0.0276	0.0160	0.0440
GOF on <i>F</i> ²	1.173	1.036	1.026

^a For all diffraction experiments, Mo K α radiation with $\lambda = 0.710\ 69\ \text{\AA}$ was used. ^b $R = \sum ||F_o| - |F_c|| / \sum |F_o|$.

are replaced by SR'. An even bigger thermodynamical instability was calculated for Te(CH₃)₄ concerning its decomposition into Te(CH₃)₂ and C₂H₆.¹⁶ Nevertheless, Te(CH₃)₄ was successfully prepared,¹⁷ and we are presently investigating a low-temperature approach toward Te(SR)₄.

Conclusion

Tellurium(IV) tetrathiolates, Te(SR)₄, are thermodynamically unstable toward decomposition into tellurium(II) dithiolates, Te(SR)₂ and S₂R₂. Structurally, Te(SR)₂ prefer conformations in which the S–C bond vector is orthogonal to the TeS₂ plane, a feature that is mainly attributed to n_p(S¹)– σ^* (Te–S²) hyperconjugation. Tellurium(II) dithiolates can decompose to Te and S₂R₂ if heated or irradiated. Te(SR)₂ exchanges ligands with Te(SR')₂ and HSR', reactions that can be used as a synthetic approach to other tellurium(II) dithiolates.

Experimental Part

General Procedures. All procedures involving Te(OⁱPr)₄ (prepared according to Denney et al.⁷) were carried out under an inert gas atmosphere or in a vacuum, using carefully dried glassware and dried solvents. Compounds **1–3** are not sensitive to moisture or air, but **3** was stored at –20 °C due to its high thermal instability.

NMR: Bruker DRX 400, B₁(¹H) = 400.0, B₁(¹³C) = 100.577, B₁(¹²⁵Te) = 126.387 MHz. Standard: TMS (¹H, ¹³C) and Te(CH₃)₂ (¹²⁵Te). IR: Mattson Galaxy 2030 FTIR, resolution 4 cm⁻¹, CsI pellets, range 4000–200 cm⁻¹. UV/vis: Zeiss Spektralphotometer DM4,

resolution 0.5 nm, quartz cuvettes, *d* = 1 cm, solutions in CCl₄, range 600–280 nm. MS: Finnigan MAT 8230, EI, 70 eV. CHS analysis: Elemental Vario EL2.

Preparation of Tellurium Di(isopropanethiolate), Te(SⁱPr)₂, **1**.

A solution of tetrakis(isopropoxy)tellurane, Te(OⁱPr)₄, (2.03 g, 5.6 mmol) in 50 mL of petroleum ether (petrol ether) was slowly added to a stirred and ice-cooled solution of isopropylthiol, HSⁱPr (1.89 g, 24.8 mmol) in 150 mL of petrol ether. After 4 h of stirring, the solvent was evaporated in vacuo from the yellow solution and the remaining yellow solid was recrystallized from methanol/petrol ether. Yield: 1.37 g (88%) of **1**; mp 35–36 °C. MS: 280[M⁺, 33.0%], 162[TeS⁺, 95], 75[SⁱPr⁺, 100]. ¹H NMR (C₆D₆): 1.23 (d, ³*J*(¹H,¹H) = 6.69 Hz, ¹*J*(¹³C,¹H) = 126 Hz, 6H, –CH(CH₃)₂), 3.00 (sept, ³*J*(¹H,¹H) = 6.70 Hz, 1H, –CH(CH₃)₂). ¹³C NMR (C₆D₆): 25.31 (–CH(CH₃)₂), 41.01 (–CH(CH₃)₂). ¹²⁵Te NMR (C₆D₆): 1025.7. UV/vis (CCl₄, 2.17 mmol L⁻¹): λ_{max} 349.2 nm, $\epsilon(\lambda_{\text{max}}) = 593\ \text{cm}^2\ \text{mmol}^{-1}$. IR: 2961(vs, $\nu_{\text{as}}(\text{CH}_3)$), 2915(s, $\nu_{\text{s}}(\text{CH}_3)$), 2859(s, $\nu(\text{CH})$), 1465(m, $\delta_{\text{as}}(\text{CH}_3)$), 1441(m, $\delta_{\text{as}}(\text{CH}_3)$), 1380(m, $\delta_{\text{s}}(\text{CH}_3)$), 1366(m, $\delta_{\text{s}}(\text{CH}_3)$), 1310(w, $\delta(\text{CH})$), 1238(vs, $\nu_{\text{as}}(\text{C}-\text{C})$), 1150(s), 1049(vs), 615(m, $\nu(\text{S}-\text{C})$), 380(s, $\nu_{\text{as}}(\text{Te}-\text{S})$), 350(w, $\nu_{\text{s}}(\text{Te}-\text{S})$). Anal. Calcd for C₆H₁₄S₂Te (fw = 277.90 g mol⁻¹): C, 25.93; H, 5.08; S 23.07. Found: C, 26.41; H, 5.53; S, 24.84.

Preparation of Tellurium Di(tertbutylthiolate), Te(S^tBu)₂, **2**.

Preparation and workup of the crude product were analogous to those of **1**, using Te(OⁱPr)₄ (4.30 g, 11.8 mmol) and *tert*-butylthiol, HS^tBu (4.76 g, 52.8 mmol). Yield: 3.23 g (89.5%) of **2**; mp 80–81 °C. ¹H NMR (C₆D₆): 1.21 (s, ¹*J*(¹³C,¹H) = 126 Hz, C(CH₃)₃). ¹³C NMR (C₆D₆): 31.7 (–C(CH₃)₃), 45.9 (–C(CH₃)₃). ¹²⁵Te NMR (C₆D₆): 906.7. UV/vis (CCl₄, 2.40 mmol L⁻¹): λ_{max} 348.7 nm, $\epsilon(\lambda_{\text{max}}) = 645\ \text{cm}^2\ \text{mmol}^{-1}$. IR: 2963(vs, $\nu_{\text{as}}(\text{CH}_3)$), 2938(m, $\nu_{\text{s}}(\text{CH}_3)$), 2920(s, $\nu_{\text{as}}(\text{CH}_3)$), 2895(s, $\nu_{\text{s}}(\text{CH}_3)$), 2859(s, $\nu_{\text{s}}(\text{CH}_3)$), 1452(s, $\delta_{\text{as}}(\text{CH}_3)$), 1393(m, $\delta_{\text{s}}(\text{CH}_3)$), + 1364(s, $\delta_{\text{s}}(\text{CH}_3)$), 1238(s, $\nu_{\text{as}}(\text{C}-\text{C})$), 1161(vs), 1125(s), 1022(m), 565(s, $\nu(\text{S}-\text{C})$), 386(s, $\nu_{\text{as}}(\text{Te}-\text{S})$), 349(s, $\nu_{\text{s}}(\text{Te}-\text{S})$). Anal. Calcd for

(16) Marsden, C. J.; Smart, B. A. *Organometallics* **1995**, *14*, 5399–5409.
(17) Gedridge, R. W., Jr.; Harris, D. C.; Higa, K. T.; Nissan, R. A. *Organometallics* **1989**, *8*, 2817–2820.

$C_8H_{18}S_2Te$ (fw = 305.95 g mol⁻¹): C, 31.41; H, 5.93; S, 20.96. Found: C, 31.41; H, 4.33; S, 18.82.

Preparation of Tellurium Di(phenylthiolate), Te(SPh)₂, 3. Preparation and workup of the crude product were analogous to those for **1**, using Te(OⁱPr)₄ (2.43 g, 6.68 mmol) and benzenethiol, HSPH (3.42 g, 31.1 mmol). Recrystallization from boiling methanol/petrol ether led to a partial decomposition. Yield: 1.58 g (68.3%) of **3**; mp 68–69 °C (dec at 75 °C). ¹H NMR (C₆D₆): 7.50 (dt, ³J(H,H) = 6.40 and 2.0 Hz, 2H, H²), 6.93 (m, 3H, H³ and H⁴). ¹³C NMR (C₆D₆): 138.4, 132.4, 128.7. UV/vis: (CCl₄, 0.60 mmol L⁻¹): λ_{max} 347.7 nm, ε(λ_{max}) = 3750 cm² mmol⁻¹. IR: 3071(w, ν(C–H)), 3050(m, ν(C–H)), 3022(sh, ν(C–H)), 1572(m), 1462(s), 1435(s), 1391(w), 1298(w), 1173(w, δ_{ip}(C–H)), 1096(w, δ_{ip}(C–H)), 1065(m, δ_{ip}(C–H)), 1020(s, δ_{ip}(C–H)), 999(w), 912(w), 741(vs, δ_{oop}(C–H)), 681(vs, ν(S–C)), 480(s, ν(Te–S)), 336(s, ν(Te–S)), 276(m), 210(m). Anal. Calcd for C₁₂H₁₀S₂Te (fw

= 345.93 g mol⁻¹): C, 41.67; H, 2.91; S 18.53. Found: C, 41.73; H, 2.14; S, 17.23.

Crystal Structure Determination. The crystal structures were solved by direct methods and difference Fourier technique (SHELXS-86);¹⁸ structural refinement was against *F*² (SHELXL-97).¹⁹ Details of the crystal structure determination of and the crystal data for **1–3** are given in Table 3.

Theoretical Methods. The ab initio calculations were performed on various servers of the Zentrum für Datenverarbeitung, Universität Mainz, on the following molecules, using the GAUSSIAN94 software package:²⁰ Te(SCH₃)₂ (C₂ symmetry), Te(SH)₂, (C₂ and C_{2v}), Te(SH)₄ (C₂ and C_{2v}), and S₂H₂ (C₂). Geometries were optimized at the Hartree–Fock level using a full-electron double-ζ basis set augmented by polarization functions (HF/3-21G(d))²¹ and with second-order Møller–Plesset perturbation theory following HF optimization with an effective core double-ζ valence basis set according to Hay and Wadt²² augmented by appropriate polarization functions for Te and S²³ (MP2/LANL2DZP). All stationary points were characterized by calculation of frequencies either from analytical second derivatives (HF/3-21g(d)) or numerically from first derivatives (MP2/LANL2DZP). Natural bond orbital analyses¹⁴ for Te(SH)₂ (C₂ and C_{2v}) and Te(SCH₃)₂ were performed with the SCF density from MP2/LANL2DZP calculations.

Acknowledgment. We thank the Fonds der Chemischen Industrie for financial support (H.F.) and the Zentrum für Datenverarbeitung, Universität Mainz, for providing the computational resources.

Supporting Information Available: The X-ray crystallographic files in CIF format for all structures presented are available on the Internet only. This material is available free of charge via the Internet at <http://pubs.acs.org>.

IC990104E

- (18) Sheldrick, G. M. SHELXS-86/SHELXTL-PC. Revision 4.1; Siemens Analytical X-ray, 1990.
- (19) Sheldrick, G. M. SHELXL-97 *Program for crystal structure refinement*; Universität Göttingen, Germany, 1997.
- (20) GAUSSIAN 94, Revision E.2. Frisch, M. J.; Trucks, G. W.; Schlegel, H. B.; Gill, P. M. W.; Johnson, B. G.; Robb, M. A.; Cheeseman, J. R.; Keith, T.; Petersson, G. A.; Montgomery, J. A.; Raghavachari, K.; Al-Laham, M. A.; Zakrzewski, V. G.; Ortiz, J. V.; Foresman, J. B.; Cioslowski, J.; Stefanov, B. B.; Nanayakkara, A.; Challacombe, M.; Peng, C. Y.; Ayala, P. Y.; Chen, W.; Wong, M. W.; Andres, J. L.; Replogle, E. S.; Gomperts, R.; Martin, R. L.; Fox, D. J.; Binkley, J. S.; Defrees, D. J.; Baker, J.; Stewart, J. P.; Head-Gordon, M.; Gonzalez, C.; Pople, J. A. Gaussian, Inc., Pittsburgh, PA, 1995.
- (21) Hehre, W. J.; Radom, L.; Schleyer, P. v. R.; Pople, J. A. *Ab Initio Molecular Orbital Theory*; Wiley: New York, 1986.
- (22) Wadt, W. R.; Hay, P. J. *J. Chem. Phys.* **1985**, *82*, 284–298.
- (23) Höllwarth, A.; Böhme, M.; Dapprich, S.; Ehlers, A. W.; Gobbi, A.; Jonas, V.; Köhler, K. F.; Stegmann, R.; Veldkamp, A.; Frenking, G. *Chem. Phys. Lett.* **1993**, *208*, 237–240.